Asian Journal of Chemistry; Vol. 36, No. 9 (2024), 2120-2128

ASIAN JOURNAL OF CHEMISTRY

https://doi.org/10.14233/ajchem.2024.32194

# Sustainable Synthesis of Silver Nanoparticles using *Epipremnum aureum* Leaf Extract: Application in Copper Ion Sensing and Antimicrobial Activity

R.K. CHAUDHARI and P.S. SHRIVASTAV*

Department of Chemistry, School of Sciences, Gujarat University, Navrangpura, Ahmedabad-380009, India

*Corresponding author: Fax: +91 79 26308057; Tel: +91 79 26300869; E-mail: pranavs@gujaratuniversity.ac.in

*Received*: 27 June 2024; *Accepted*: 29 July 2024; *Published online*: 30 August 2024; AJC-21738

This work presents a sustainable approach to produce silver nanoparticles (AgNPs) using extracts from *Epipremnum aureum* leaves under ambient conditions without the use of toxic chemicals. Various analytical techniques such as UV-visible, FTIR, powder XRD, EDX, HRTEM, SEM and TGA were employed to characterize the prepared AgNPs. The synthesized AgNPs were spherical with sizes ranging from 5.72 nm to 30.33 nm and exhibited a surface plasma resonance at 419 nm. The presence of Ag was ascertained using EDX spectroscopy. The optical band gap of AgNPs was 2.17 eV, which showed effective antimicrobial activity compared to $AgNO_3$ solution. Using AgNPs, the agar-well diffusion method showed high antimicrobial activity against *Bacillus subtilis* and *Escherichia coli* compared to the disc diffusion method. The prepared AgNPs were successful in detecting selectively $Cu^{2+}$ ion within 1 min with a limit of detection of 0.1 mg/L.

**Keywords: Antimicrobial activity, Copper ion, *Epipremnum aureum*, Silver nanoparticles.**

## INTRODUCTION

Nanotechnology is an emerging scientific discipline dedicated to creating and utilizing tiny structures at the nanoscale, possessing distinctive chemical and physical characteristics. It encompasses the measurement, assembly, monitoring and synthesis of materials within the range of 1 to 100 nm [1]. This discipline has made a profound impact on diverse sectors, including biomedical, chemical industries, catalysis, drug delivery, energy science, electronics, optics, wastewater treatment, optoelectronic devices, nonlinear optical devices, photochemical applications and space industries [2,3]. Nanoparticles are widely utilized in these contexts because of their elevated surface area compared to their larger counterparts, distinguishing them from bulk materials [4]. Various physical, chemical and electrochemical methods are employed for the synthesis of nanoparticles [5]. However, these approaches typically necessitate a substantial amount of electrical and energy-related machinery, as well as the use of toxic and hazardous chemicals, occasionally resulting in the generation of harmful byproducts [6]. To address these challenges, researchers have developed an environmentally friendly approach known as "Green synthesis" [7,8]. This method not only conserves energy and resources but also ensures the safety and biocompatibility of the environment [4]. In green synthesis, various biological entities such as fungi, bacteria, algae and plants serve as primary agents for production of nanoparticles [9]. While the use of microorganisms in nanoparticles synthesis demands the maintenance of sterile conditions, the preparation of suitable culture media and the viability of the chosen strain, these requirements can diminish the appeal of this method. As a result, researchers are increasingly turning to plant based approaches for nanoparticles synthesis [10].

India boasts rich biodiversity, making the procurement of plants straightforward [11]. The utilization of plants in nanoparticles synthesis proves to be both cost-effective and sustainable. Furthermore, it eliminates the risk of generating toxic byproducts [12]. Nanoparticles produced through plant-based methods exhibit enhanced stability and a faster production rate compared to microorganisms [13]. Notably, certain plants and their extracts facilitate the rapid reduction of metal ions to their zero-valent state, surpassing the capabilities of bacteria and fungi [14]. Consequently, researchers have gravitated towards the use of plants in nanoparticle synthesis [15]. Plants encompass various components, including leaves, flowers, fruits, barks and roots, all of which serve as vital resources for synthesizing different metal and metal oxide nanoparticles [15]. For instance,

the leaf of *Dalbergia sissoo* is used for generating magnesium oxide nanoparticles [6], while *Saraca indica* flowers are employed in silver nanoparticles synthesis [16]. *Duranta erecta* fruits have contributed towards copper nanoparticles production [17], *Eucommia ulmoides* barks have yielded palladium nanoparticles [18] and the roots of *Berberis vulgaris* have been harnessed for silver nanoparticles creation [19]. Phytochemicals found in plants, including flavonoids, terpenoids and polyphenols, which contain diverse functional groups, are crucial for reducing metal ions biologically. Additionally, these phytochemicals create a protective coating around the synthesized nanoparticles, effectively preventing their aggregation and enhancing nanoparticle stability [9]. The dimensions of nanoparticles are impacted by various factors such as pH levels, the concentration of plant extracts and metal ions, as well as temperature. By meticulously optimizing these parameters, we achieve the synthesis of well-defined and controlled nanoparticles [6].

Silver nanoparticles (AgNPs) have attracted considerable attention due to their exceptional stability [20], thermal [21] and optical characteristics [22], high electrical conductivity [23] and catalytic properties [24]. They have diverse applications across various industries, including food, healthcare, cosmetics, biosensors, cryogenic superconductors, composite fibers, electronic components and the photocatalytic degradation of organic dyes, making them a focal point of extensive research [25,26]. AgNPs have been successfully synthesized from a range of plants, including Tulsi [27], *Adhatoda vasica* [28], *Zanthoxylum armatum* [29], *Psidium guajava L* [30], *Salvia officinalis* [31], *Nicotiana tobaccum* [32], *Scutellaria barbata* [33] and *Conocarpus lancifolius* [34].

Water serves as a universal solvent and holds vital importance for the human body. Unfortunately, it is currently facing pollution due to chemical and microbial contamination resulting from industrialization and the high population density [35]. Contaminated water often contains harmful bacteria, including *Escherichia coli*, *Salmonella typhi*, *Salmonella paratyphi*, *Helicobacter pylori* and *Campylobacter jejuni*. Among these, *E. coli* is frequently found in contaminated water sources and is responsible for causing conditions such as diarrhoea and Hemolytic Uremic Syndrome (HUS) [36].

*Epipremnum aureum*, a member of the plant kingdom and the Araceae family, is commonly known as golden pothos, devil's ivy, money plant, silver vine or taro vine [37]. It contains a diverse array of phytochemicals and compounds, including tannins, cardiac glycosides, steroidal terpenoids, saponins, saponin glycosides, anthraquinones, flavonoids, phenols, alkaloids, quercetin dihydrate, ferulic acid, cinnamic acid and caffeic acid [38]. *Epipremnum aureum* exhibits antibacterial, antitermite, antioxidant and defluoridation properties [38,39]. In present work, we utilized extracts from *Epipremnum aureum* leaves to produce AgNPs at ambient temperature. These nanoparticles were then analyzed using various analytical methods such as UV-visible spectroscopy, Fourier-transform infrared spectroscopy (FTIR), powder X-ray diffraction (XRD), energy dispersive X-ray analysis (EDXA), high-resolution transmission electron microscopy (HRTEM), scanning electron microscopy (SEM) and thermogravimetric analysis (TGA). Additionally, the antimicrobial activity of the AgNPs was explored against *E. coli* through agar well diffusion and disc diffusion methods. Furthermore, a range of metals ions were selected for testing the sensing properties of the green synthesized NPs.

## EXPERIMENTAL

Leaves of *Epipremnum aureum* (Fig. 1) were collected from Vastral (N23°2′18.3768; E72°32′34.8468) region of Ahmedabad, India during the summer season. Analytical grade silver nitrate ($AgNO_3$, 99%) was purchased from Finar Limited; Gujarat, India and nutrient agar powder was obtained from Himedia Laboratories Limited, India. Milli Q water was used at different stages of this study. Additionally, all other chemicals utilized in the study were of analytical grade.

Fig. 1 Leaves of *Epipremnum aureum*

**Characterization:** Green-synthesized AgNPs were analyzed by Jasco V-630 UV-visible spectrophotometer (Kyoto, Japan) in the range of 200 to 800 nm. Using this data, the maximum absorption wavelength and band gap of synthesized AgNPs were evaluated. FTIR from Agilent Micro Lab, United States was used to identify the functional groups responsible for the synthesis of AgNPs and for the capping and stabilizing functional groups present on the surface of AgNPs. It was recorded from 4000 to 400 $cm^{-1}$ wavenumber. XRD (Rigaku smart lab, Japan) provided an idea regarding the phase and crystalline structure of AgNPs. It was operated at a voltage of 40 kV and an electric current of 45 mA with Cu $K\alpha$ radiation and a scanning rate of 2º/min within a range of 5º to 80º. The average crystalline size of AgNPs was calculated from the XRD data using Debye Scherrer's formula. The EDAX (Carl Zeiss supra55, Japan) was used to evaluate the qualitative elemental analysis of AgNPs. The HRTEM (Jeol Jem 2100 plus, Japan) provided the size and shape of AgNPs. The surface morphology of AgNPs was examined using SEM (Hitachi SU70 SEM, Japan) operated at 15 kV. Thermal characterization and decomposition pattern of AgNPs were obtained by a thermogravimetric analyzer (TGA, NETZSCH STA 2500, India). This instrument was operated between 30-1000 ºC under a nitrogen atmosphere at a heating rate of 10 ºC/min.

**Aqueous leaf extract of *Epipremnum aureum*:** The fresh, undamaged green leaves of *E. aureum* were initially rinsed with tap water and then with purified Milli Q water. Thereafter, 25 g of leaves were chopped into small pieces and placed in a 250 mL glass beaker. Subsequently, 100 mL of Milli Q water was added and the mixture was heated on a hot plate at 60 ºC for 50 min. The solution was filtered using Whatman filter paper no. 41 having a pore size ranging from 20-25 µm. The resulting solution obtained from the leaves exhibited a light-yellow colour and was utilized as a medium for reducing, capping and stabilizing $AgNO_3$ solution. The extract was then refrigerated at 4 ºC to mitigate any impacts associated with moisture.

**Preparation of AgNPs using *E. aureum* leaf extract:** A 0.01 M solution of $AgNO_3$ was made using Milli Q water and a 50 mL portion was put into a conical flask. To prevent light-induced reactions, the flask was covered with aluminum foil due to the sensitive nature of $AgNO_3$. Then, *E. aureum* leaf extract was slowly added to the solution while stirring continuously at 480 rpm. The addition of 10-12 mL of extract afforded a colour change from clear to brown, implying the formation of AgNPs. For purification, the solution containing these biogenically synthesized AgNPs was centrifuged at 6000 rpm for 20 min to obtain a clear supernatant. The supernatant was removed and the remaining pellet was washed three times with Milli Q water. Thereafter, the pellet was dried overnight at room temperature and used for further characterization and analysis.

### Antimicrobial activity

**Preparation of nutrient agar plate:** In a 250 mL conical flask, 2.8 g of nutrient agar powder was dissolved in 100 mL of Milli-Q water. The pH of the solution was 7.6. The mouth of flask was sealed with cotton and wrapped with paper. The flask mixture underwent sterilization through autoclaving at 15 pounds per square inch pressure and 121 ºC for 20 min. After sterilization, 20 mL of mixture were transferred into individual 90 mm sterile petri dishes and left to solidify at the ambient temperature.

**Agar well diffusion and disc diffusion method:** *E. coli* (Gram-negative) bacterial cultures were obtained from S.S.M.C.A. Science College, Ahmedabad, India. In agar well diffusion method [40], a hole was created at the center of each petri dish using a cup borer and 30 µL of AgNPs (15 µg/mL) were carefully added into it. Meanwhile, in the disc diffusion method [41], sterile forceps were used to immerse a disc into 30 µL of AgNPs (15 µg/mL) and the disc was then placed in the center of the petri dish. Streptomycin served as the positive control in these experiments. Each set of plates underwent a 24 h incubation period at 37 ºC. The experiments were replicated three times and the diameter of the inhibition zones were measured in mm. Different concentrations of AgNPs were employed to ascertain the minimum inhibitory concentration (MIC) for *E. coli* bacteria.

**Sensing of $Cu^{2+}$ ions:** Green-synthesized AgNPs were employed as nanosensor to detect $Cu^{2+}$ ions. AgNPs were subjected to testing against a range of metal ions, including $Cu^{2+}$, $Na^{+}$, $Cd^{2+}$, $Sr^{2+}$, $Mg^{2+}$, $Ba^{2+}$, $Al^{3+}$, $Fe^{2+}$ and $Co^{2+}$. In this procedure, 4 mL AgNPs solution served as the test sample and 1 mL aliquot of 25 mg/L salt solution containing the metal ions was added to the AgNPs solution. Additionally, 1 mL of Milli-Q water was employed as control. Both the control and test samples were left at room temperature for 1 min. The results were easily discerned by the naked eye, comparing the colour of the control and test samples. Different concentrations of $Cu^{2+}$ ions ranging from 10 mg/L to 0.001 mg/L were utilized to establish the limit of detection for $Cu^{2+}$ ions.

## RESULTS AND DISCUSSION

**Optimization of reaction parameters:** The volume of *Epipremnum aureum* leaf extract, the concentration of $AgNO_3$, the pH of AgNPs solution and temperature play crucial roles in influencing the bioreduction process. Therefore, it is essential to establish optimal conditions for these parameters when preparing AgNPs.

**Volume of *E. aureum* leaf extract:** The effect of volume of *E. aureum* leaf extract was examined by utilizing different volumes, specifically 5, 10, 15, 20 and 25 mL, for 50 mL of 0.01 M $AgNO_3$ solution and observed the changes through the UV-visible spectral analysis.The experiment revealed that 5 mL amount of leaf extract was insufficient to convert $Ag^{+}$ ions into $Ag^{0}$, as due to the absence of a clear absorption peak in the AgNPs spectra (Fig. 2a). When the volume of leaf extract was raised to 10-15 mL range, a large amount of small-sized AgNPs were formed. However, when the volume exceeded 15 mL, the production of very small-sized AgNPs occurred. These nanoparticles tended to aggregate, giving rise to larger-sized AgNPs, ultimately causing the absorption peak to shift from 422 to 464 nm. Considering these findings, it was determined that the optimum volume of leaf extract for this green synthesis process was between 10-15 mL.

**Concentration of $AgNO_3$:** The effect of $AgNO_3$ concentration was studied systematically by varying the concentration from 0.001 M to 2 M, while maintaining all other variables constant. The absorption peak of AgNPs, formed with $AgNO_3$ concentrations ranging from 0.001 M to 0.1 M, exhibited a consistent range, falling between 411 nm to 419 nm (Fig. 2b). However, at concentrations of 1 M and 2 M, the absorption peak shifted to 447 nm and 452 nm, respectively. This observation suggests a clear correlation between the wavelength maxima ($\lambda_{max}$) and particle size, with both parameters increasing when the concentration of $AgNO_3$ is increased. This behaviour agrees with the findings reported by Aryan *et al*. [42]. Based on these results, the optimal concentration range for $AgNO_3$ in this green synthesis process lies between 0.001M and 0.1M.

**Effect of pH:** The optimal pH was investigated spectrophotometrically by varying the pH values from 3-11. The absorption peak of AgNPs was observed at 424 nm up to a pH of 5, beyond which a red shift occurred (Fig. 2c). This suggests an increase in the particle size of AgNPs with an elevated pH. Based on these findings, a pH range of 3-5 was identified as favourable for the green synthesis. The acidic nature of flavonoids, terpenoids, phenols and certain acids in the leaf extract was diminished at higher pH levels. As a result, the greater presence of hydroxyl ions in the solution promoted the clustering of particles rather than their reduction [6].

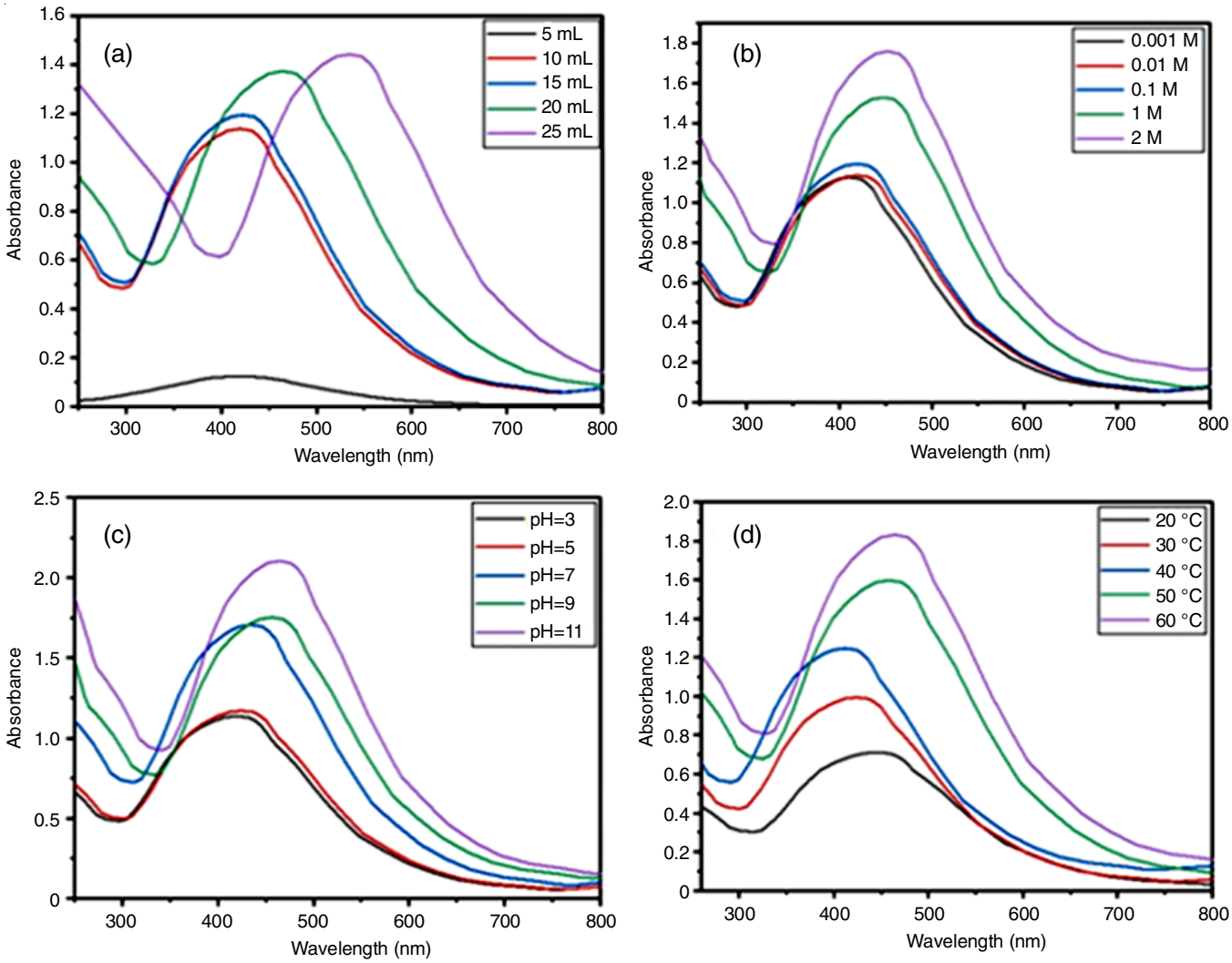


Fig. 2. Absorption spectra of *E. aureum* leaves extract mediated AgNPs at different (a) volume of leaf extract, (b) concentration of $AgNO_3$, (c) pH of reaction mixture and (d) temperature

**Effect of temperature:** The synthesis of AgNPs can be enhanced by optimizing the temperature, ranging from 20 to 60 ºC, while maintaining other variables constant. The optimum temperature was determined from the absorption spectra of AgNPs. With an increase in temperature from 20 to 40 ºC, the absorption peak exhibited a blue shift, moving from 444 nm to 411 nm (Fig. 2d), which suggests a reduction in the size of AgNPs at a specific temperature. The elevated temperature led to a higher rate of reaction, attributed to increased kinetic energy, indicating a rise in the formation of smaller-sized AgNPs [43]. In the temperature range of 40-60 ºC, the absorption peak displayed a red shift, transitioning from 411 nm to 462 nm. At higher temperatures, the phytochemicals from the leaf extract in solution may break down, hindering their ability to completely reduce $AgNO_3$ and stabilize AgNPs. Consequently, particle aggregation occurs, leading to an increase in particle size [6].

**Stability of green synthesized AgNPs:** The stability of synthesized AgNPs was assessed by analyzing their absorption spectra over a 5 week period. Fig. 3 indicates that there was no significant alteration in the absorption peak of AgNPs within the initial 3 weeks. However, a slight increase in $\lambda_{max}$ was observed after the 3rd week and a prominent change became apparent after the 4th week. Consequently, the AgNPs remained stable for up to 4 weeks, but beyond this point, aggregation

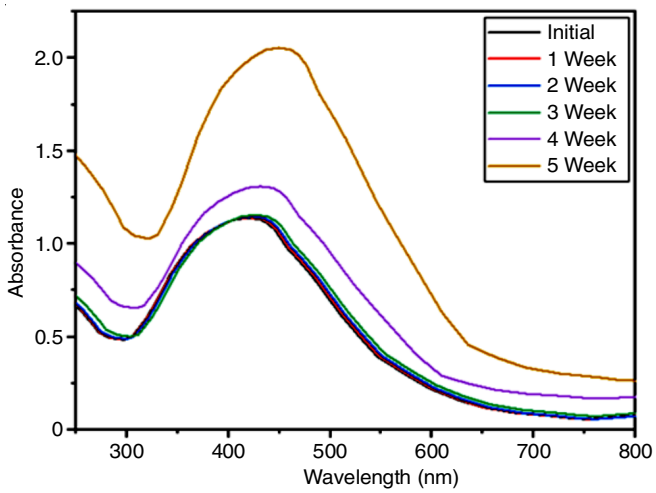


Fig. 3. UV-visible spectra of *E. aureum* leaves extract mediated AgNPs at different time duration

led to an increase in particle size. This observation suggests that the synthesized AgNPs showed significant stability due to the inclusion of capping and stabilizing agents found in the leaf extract.

**UV-visible spectra:** The absorption peak of the green-synthesized AgNPs was observed at 419 nm (Fig. 4). Consistent with prior findings, AgNPs typically exhibit absorption peaks within the range of 410 nm to 430 nm [44]. The leaf extract of *E. aureum* displayed an absorption peak at 326 nm. UV-visible spectra of AgNPs were utilized in Tauc plot analysis to determine the energy gap ($E_g$) or band gap. The $E_g$ value of AgNPs was determined by plotting $(\alpha h\nu)^2$ against $h\nu$, where $h\nu$ represents energy and $\alpha$ stands for the absorptivity coefficient. By extrapolating a tangent of curve on the *x*-axis, the $E_g$ value was obtained (Fig. 5). Nanoparticles with a lower $E_g$ value are known to display better antibacterial activity than those with a higher $E_g$ value [6] and it was found that in this work, *E. aureum* mediated AgNPs had an $E_g$ value of 2.17 eV.

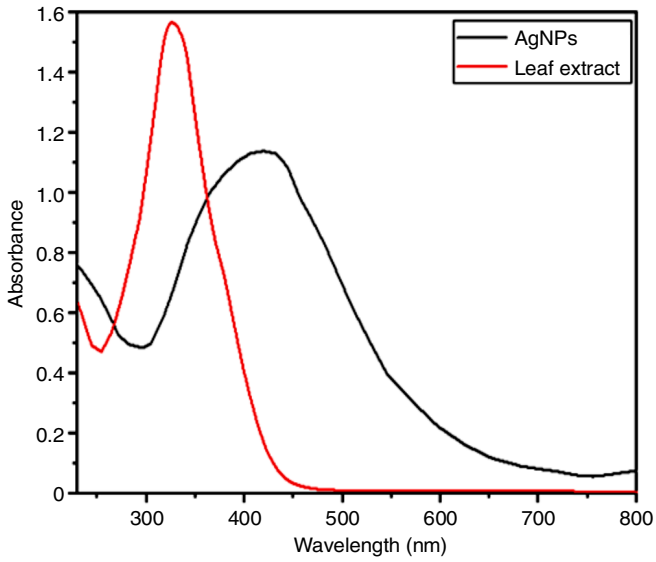


Fig. 4. UV-visible spectra of AgNPs and *E. aureum* leaves extract

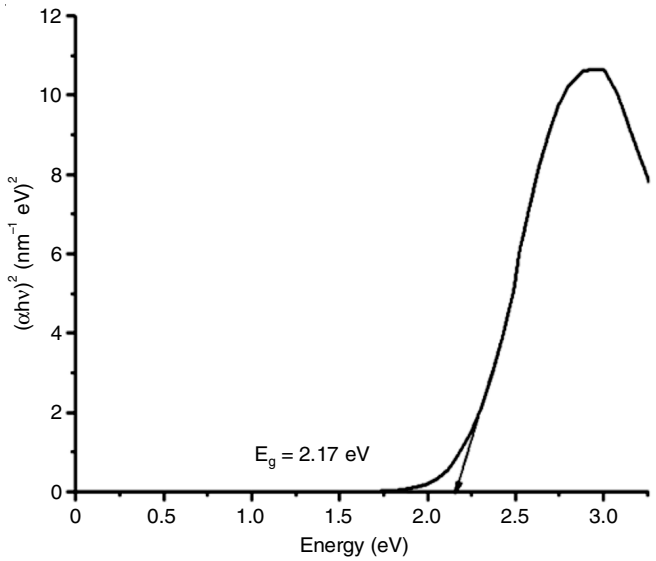


Fig. 5. Tauc plot of *E. aureum* leaves extract mediated AgNPs

**FTIR spectra:** Fig. 6 displays the FTIR spectra of both the leaf extract of *E. aureum* and the synthesized AgNPs. Within the leaf extract, significant vibrational peaks were observed at various wavenumbers, including 3317.33 cm$^{-1}$ for the –OH stretching vibration, 2918.50 cm$^{-1}$ for C-H stretching (aliph.), 2851.41 cm$^{-1}$ for –NH (amine group) stretching, 1610.21 cm$^{-1}$ for C=O stretching, 1412.66 cm$^{-1}$ for C=C bond (arom.) stretching, 1326.93 cm$^{-1}$ for C-N stretching (arom. amine), 1013.83 cm$^{-1}$ for -COO- (anhydride group) stretching and 872.19 cm$^{-1}$ for C=C bending (alkene). In the FTIR spectrum of synthesized AgNPs, peaks at 2918.56 cm$^{-1}$, 2851.41 cm$^{-1}$ and 1013.83 cm$^{-1}$ were reminiscent of those in the leaf extract, albeit with comparatively lower absorption peak intensities. However, certain peaks in the *E. aureum* leaf extract appeared to have shifted in the AgNPs synthesized *via* green methods, specifically, from 3317.331 cm$^{-1}$ to 3291.239 cm$^{-1}$ and from 1610.21 cm$^{-1}$ to 1625.119 cm$^{-1}$. In green synthesis, same functional groups and shifted peaks were found as capping and stabilizing agents [31]. Several certain peaks, such as 1412.661 cm$^{-1}$, 1326.932 cm$^{-1}$ and 872.197 cm$^{-1}$, were absent in the FTIR spectrum of AgNPs, indicating the utilization of these functional groups in the reduction process of $Ag^+$ ions.

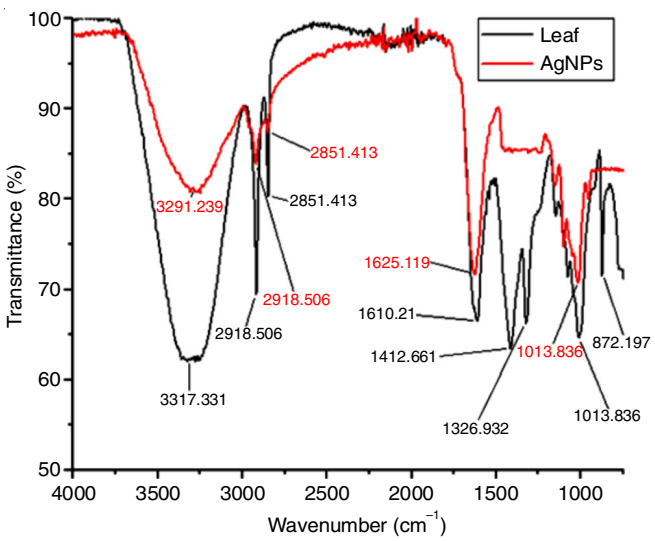


Fig. 6. FTIR spectra of *Epipremnum aureum* leaves extract and AgNPs

**XRD spectra:** The XRD spectrum for green-synthesized AgNPs is depicted in Fig. 7, revealing significant diffraction peaks at 21.99º, 29.68º, 32.34º, 38.39º, 41.08º, 44.36º, 46.32º, 51.76º, 57.61º, 64.62º, 67.57º and 77.54º correspond to (2 1 1), (2 1 0), (3 1 1), (4 1 1), (4 2 0), (4 2 2), (4 3 1), (4 4 0), (6 2 0), (4 4 4), (6 4 0) and (8 1 1) planes, respectively. These peaks suggest a face-centered cubic structure [45]. The diffraction peaks of AgNPs align with the JCPDS data [File card no.: 96-101-005]. The lattice parameters, with $a = b = c = 9.99$ Å and $\alpha = \beta = \gamma = 90º$, further confirm the face-centered cubic structure of AgNPs [46]. In nanoscience, particle size is a crucial parameter. Scherrer's formula (eqn. 1), utilizing the full width half maximum (FWHM) of peak, was employed to determine the particle size, emphasizing its significance in the analysis [47].

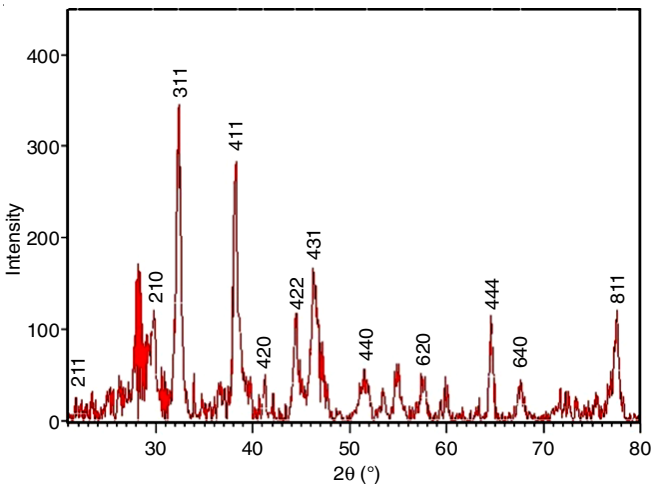


Fig. 7. XRD spectra of *E. aureum* leaves extract mediated AgNPs

TABLE-1
XRD DATA OF AgNPs PREPARED FROM LEAVES EXTRACT OF *Epipremnum aureum*

| 2θ (°) | d-spacing (Å) | Crystalline size (nm) | Strain ε (× $10^{-4}$) ($Lin^{-2}$ $m^{-4}$) |
|---|---|---|---|
| 21.9905 | 4.04208 | 5.798854 | 3.485238 |
| 29.6872 | 3.00934 | 9.434219 | 1.594907 |
| 32.3403 | 2.76826 | 11.88271 | 1.164829 |
| 38.3943 | 2.34456 | 8.041695 | 1.457750 |
| 41.0880 | 2.19686 | 12.18761 | 0.901268 |
| 44.3659 | 2.04186 | 12.32489 | 0.828350 |
| 46.3254 | 1.95996 | 12.41339 | 0.789453 |
| 51.7646 | 1.76608 | 10.13642 | 0.871157 |
| 57.6163 | 1.59986 | 13.02645 | 0.614080 |
| 64.6204 | 1.44234 | 13.50743 | 0.533908 |
| 67.5753 | 1.38629 | 13.73715 | 0.504576 |
| 77.5455 | 1.23107 | 14.64985 | 0.420165 |

$$\tau = \frac{k\lambda}{\beta_{2\theta}\cos\theta} \quad (1)$$

where τ denotes the thickness of crystallite measured perpendicularly to the reflecting plane; k stands for Scherrer's constant (taken as 0.9 for spherical particles); λ represents the wavelength of X-ray radiation (1.5405 Å); $\beta_{2\theta}$ indicates the width at half the maximum intensity measured in radians and θ corresponds to Bragg's angle [45]. The size of AgNPs ranged from 5.79 nm to 14.64 nm, varying with the type of reflection used. The average size of the crystalline AgNPs was found to be 11.42 nm, aligning with the results from HRTEM. Data for lattice strain and *d*-spacing were computed using a modified Scherrer's formula [48], as shown in Table-1.

**Morphology studies:** The HRTEM micrograph (Fig. 8a) revealed that the AgNPs displayed a size range of 5.72 to 30.33 nm, with an average particle size of 13.40 nm. The particles were spherical in shape and the range of their sizes is depicted visually in the histogram provided alongside (Fig. 8b). The SAED pattern yielded insights into the crystalline properties of the synthesized AgNPs, revealing diffraction rings interspersed with dots, signifying their crystalline arrangement (Fig. 8c). EDAX spectroscopy was utilized to determine the elemental composition of the synthesized AgNPs. A distinct peak at 3 keV verified the existence of silver within the AgNPs (Fig. 9a). Additionally, the detection of carbon and oxygen in EDAX suggested the capping and stabilizing nature of phytochemicals on the surface of AgNPs. The SEM micrograph illustrated some irregular spherical shape of AgNPs (Fig. 9b), further supporting the particle shape observed in the HRTEM analysis.

**Thermal studies:** Thermal stability and mass loss of green synthesized AgNPs were evaluated through TGA analysis. The thermogram (Fig. 10) indicates an initial mass loss of 12.76% between 98 ºC and 250 ºC, attributed to the evaporation of water molecules present on the surface of AgNPs. A subsequent mass loss of 20.01% was observed up to 827 ºC, resulting from the decomposition and evaporation of phytochemicals acting as capping and stabilizing agents on the surface of AgNPs. Beyond 827 ºC, the mass percentage of AgNPs stabilized at around 66%, indicating no further mass loss on account of the silver metal.

**Antimicrobial activity:** The green synthesized AgNPs were assessed for antimicrobial activity against Gram-negative bacteria *E. coli*. The results (Table-2) demonstrated an considerably larger zone of inhibition (ZOI) for AgNPs when using the agar well diffusion methodology in comparison to the disc diffusion method. In contrast, the leaf extract of *E. aureum*, which inherently possesses antimicrobial activity, displayed a smaller ZOI. The superior antimicrobial efficacy of small-sized AgNPs, compared to $AgNO_3$, is attributed to their ability to

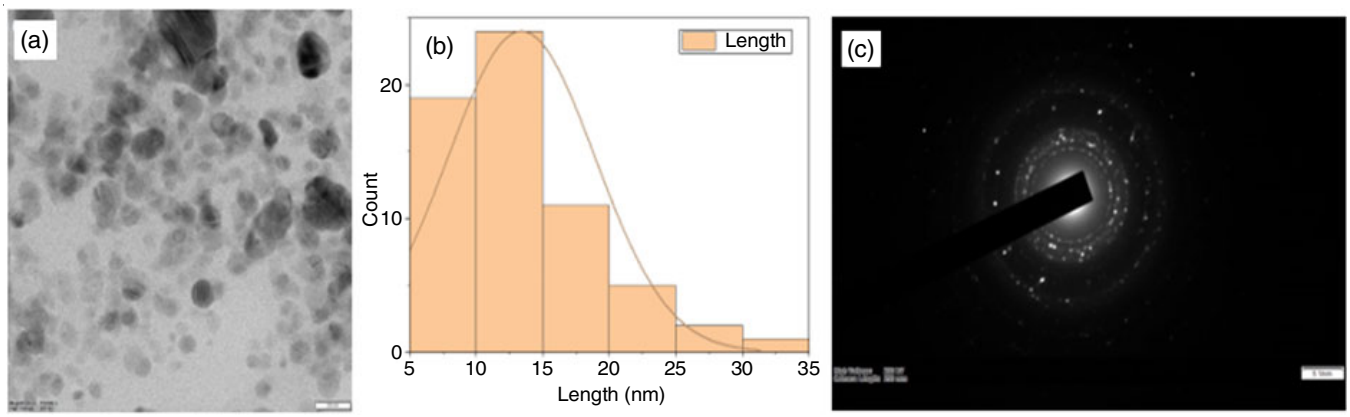


Fig. 8. (a) HRTEM image, (b) distribution of particle size and (c) SAED pattern of *E. aureum* leaves extract mediated AgNPs

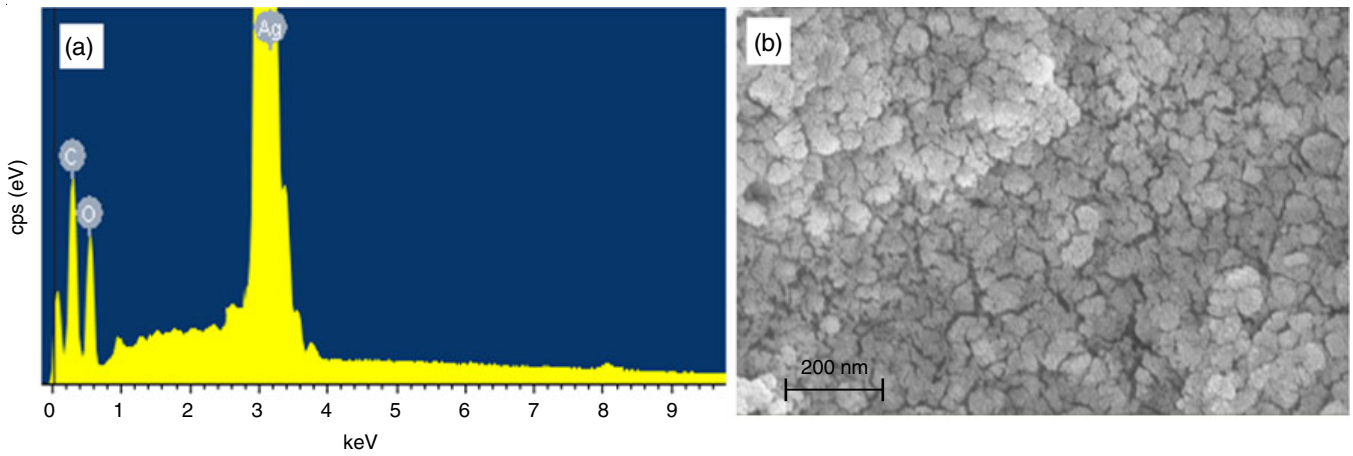


Fig. 9. (a) EADX pattern and (b) SEM micrograph of *E. aureum* leaves extract mediated AgNPs

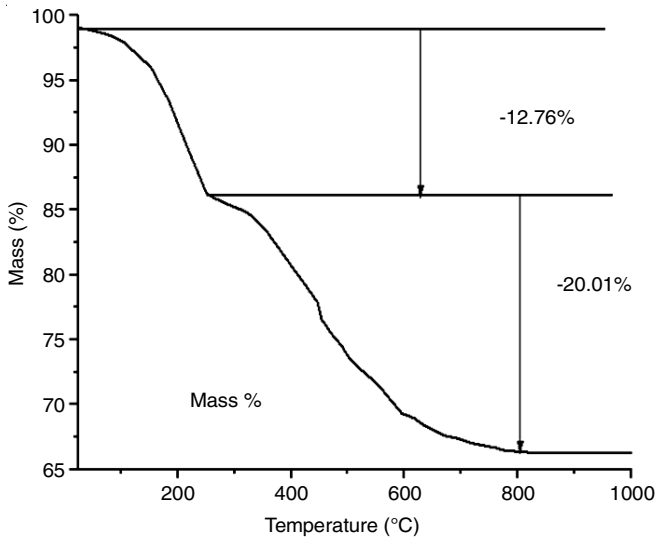


Fig. 10. Thermogram of *E. aureum* leaves extract mediated AgNPs

TABLE-2
RESULTS FOR ZOI OF DIFFERENT SAMPLES

| Sample name | Concentration (µg/mL) | Volume (µL) | ZOI (mm) |
|---|---|---|---|
| AgNPs (agar well diffusion) | 15 | 30 | 28 ± 0.6 |
| AgNPs (disc diffusion) | 15 | 30 | 20 ± 0.3 |
| $AgNO_3$ | 15 | 30 | 16 ± 0.4 |
| Leaf extract | – | 30 | 2.3 ± 0.5 |
| Streptomycin | 15 | 30 | 41 ± 1.0 |

penetrate a larger extent of cells, resulting in a more substantial ZOI [42]. Despite maintaining identical AgNPs concentrations in both agar well diffusion and disc diffusion methods, the former yielded a larger ZOI. This disparity could be due to the direct addition of AgNPs into the well in the agar well diffusion method, ensuring effective spread. On the other hand, in the disc diffusion method, the discs are immersed in AgNPs prior to being placed on the agar surface. The AgNPs were tested against *E. coli* in concentrations ranging from 15 µg/mL to 0.94 µg/mL to determine the MIC. As indicated in Table-3, the ZOI is lowered with decreasing AgNPs concentration.

TABLE-3
ZOI AT DIFFERENT CONCENTRATION
OF AgNPs HAVING SAME VOLUME

| Conc. (µg/mL) | 15 | 7.5 | 3.75 | 1.87 | 0.94 |
|---|---|---|---|---|---|
| ZOI (mm) | 28±0.6 | 13.2±0.7 | 5.9±0.3 | 2.2±0.3 | 0.0 |

**Sensing of $Cu^{2+}$ ions:** This study assesses the application of green synthesized AgNPs as a sensor for detecting $Cu^{2+}$ ions. The specificity of AgNPs for $Cu^{2+}$ was examined by comparing the colour changes in the reaction mixture with other metal cations including $Na^+$, $Cd^{2+}$, $Sr^{2+}$, $Mg^{2+}$, $Ba^{2+}$, $Al^{3+}$, $Fe^{2+}$ and $Co^{2+}$ (Fig. 11). The reaction mixture of $Cu^{2+}$ ions and AgNPs exhibited a distinct change in colour from brown to greenish blue. With a reduction potential of 0.80 volt for $Ag^+$ and 0.34 volt for $Cu^{2+}$, it is clear that this color change is not due to a redox

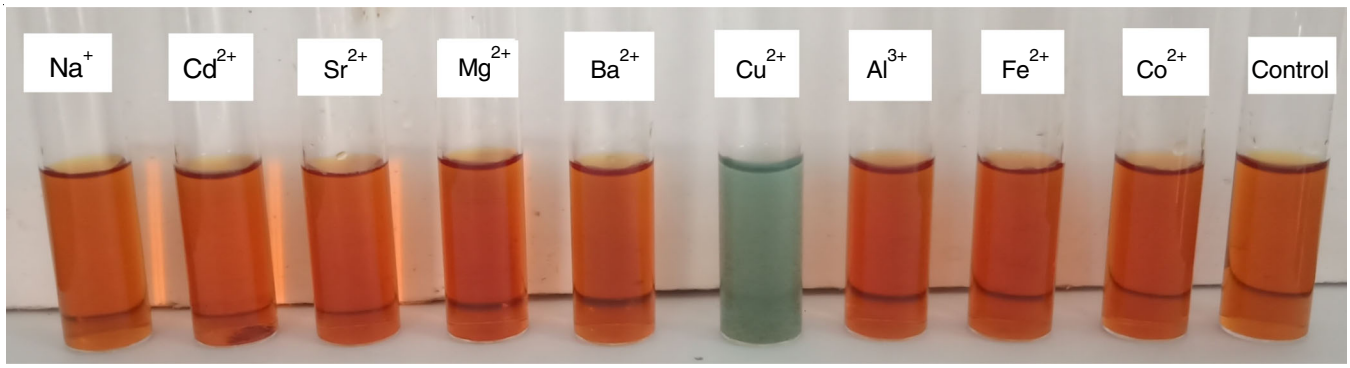


Fig. 11. Images of reaction between *E. aureum* leaves extract mediated AgNPs with different metal ions

process. Since AgNPs contain the reduced form of $Ag^0$, further reduction is not feasible. The observed colour change is attributed to the complex formation between AgNPs and $Cu^{2+}$ [49]. However, no colour change was observed for other metal cations. These results demonstrated that the method is highly selective for $Cu^{2+}$ ions using the synthesized AgNPs, with a limit of detection of 0.1 mg/L.

## Conclusion

This study presents a sustainable method for synthesizing AgNPs using *Epipremnum aureum* leaf extract and characterized. This approach delivers good antibacterial action against *E. coli* with synthesized AgNPs and also display the colourimetric sensing capabilities for $Cu^{2+}$ ions with high selectivity and sensitivity.

## CONFLICT OF INTEREST

The authors declare that there is no conflict of interests regarding the publication of this article.

## REFERENCES


1. M. Napagoda, D. Jayathunga and S. Witharana, Introduction to Nanotechnology. In: Nanotechnology in Modern Medicine, Springer Nature, Singapore, p. 1-17 (2023).
2. M. Nasrollahzadeh, S.M. Sajadi, M. Sajjadi and Z. Issaabadi, *Interf. Sci. Technol.*, **28**, 1 (2019); https://doi.org/10.1016/B978-0-12-813586-0.00001-8
3. V. Chavda, B. Patel, S. Singh, D. Hirpara, V.D. Rajeswari and S. Kumar, *RSC Sustainability*, **1**, 2038 (2023); https://doi.org/10.1039/D3SU00236E
4. S. Jadoun, R. Arif, N.K. Jangid and R.K. Meena, *Environ. Chem. Lett.*, **19**, 355 (2021); https://doi.org/10.1007/s10311-020-01074-x
5. C. Vauthier and K. Bouchemal, *Pharm. Res.*, **26**, 1025 (2009); https://doi.org/10.1007/s11095-008-9800-3
6. M.I. Khan, M.N. Akhtar, N. Ashraf, J. Najeeb, H. Munir, T.I. Awan, M.B. Tahir and M.R. Kabli, *Appl. Nanosci.*, **10**, 2351 (2020); https://doi.org/10.1007/s13204-020-01414-x
7. A. Gour and N.K. Jain, *Artif. Cells Nanomed. Biotechnol.*, **47**, 844 (2019); https://doi.org/10.1080/21691401.2019.1577878
8. I. Hussain, N.B. Singh, A. Singh, H. Singh and S.C. Singh, *Biotechnol. Lett.*, **38**, 545 (2016); https://doi.org/10.1007/s10529-015-2026-7
9. E. Nagaraj, P. Shanmugam, K. Karuppannan, T. Chinnasamy and S. Venugopal, *New J. Chem.*, **44**, 2166 (2020); https://doi.org/10.1039/C9NJ04961D
10. S. Hamedi and S.A. Shojaosadati, *Polyhedron*, **171**, 172 (2019); https://doi.org/10.1016/j.poly.2019.07.010
11. T. Vattakaven, R.M. George, D. Balasubramanian, M. Réjou-Méchain, G. Muthusankar, B.R. Ramesh and R. Prabhakar, *Biodivers. Data J.*, **4**, e10279 (2016); https://doi.org/10.3897/BDJ.4.e10279
12. N. Khatoon, R. Ahmad and M. Sardar, *Biochem. Eng. J.*, **102**, 91 (2015); https://doi.org/10.1016/j.bej.2015.02.019
13. N.T.T. Nguyen, L.M. Nguyen, T.T.T. Nguyen, T.T. Nguyen, D.T.C. Nguyen and T.V.V. Tran, *Environ. Chem. Lett.*, **20**, 2531 (2022); https://doi.org/10.1007/s10311-022-01425-w
14. S. Iravani, *Green Chem.*, **13**, 2638 (2011); https://doi.org/10.1039/c1gc15386b
15. G. Oza, A. Reyes-Calderón, A. Mewada, L.G. Arriaga, G.B. Cabrera, D.E. Luna, H.M. Iqbal, M. Sharon and A. Sharma, *J. Mater. Sci.*, **55**, 1309 (2020); https://doi.org/10.1007/s10853-019-04121-3
16. V.K. Vidhu and D. Philip, *Spectrochim. Acta A Mol. Biomol. Spectrosc.*, **117**, 102 (2014); https://doi.org/10.1016/j.saa.2013.08.015
17. M. Ismail, S. Gul, M.I. Khan, M.A. Khan, A.M. Asiri and S.B. Khan, *Green Process. Synth.*, **8**, 135 (2019); https://doi.org/10.1515/gps-2018-0038
18. L. Duan, M. Li and H. Liu, *IET Nanobiotechnol.*, **9**, 349 (2015); https://doi.org/10.1049/iet-nbt.2015.0020
19. M. Behravan, A. Hossein Panahi, A. Naghizadeh, M. Ziaee, R. Mahdavi and A. Mirzapour, *Int. J. Biol. Macromol.*, **124**, 148 (2019); https://doi.org/10.1016/j.ijbiomac.2018.11.101
20. C. Levard, E.M. Hotze, G.V. Lowry and G.E. Brown Jr., *Environ. Sci. Technol.*, **46**, 6900 (2012); https://doi.org/10.1021/es2037405
21. J. Sun, D. Ma, H. Zhang, X. Liu, X. Han, X. Bao, G. Weinberg, N. Pfänder and D. Su, *J. Am. Chem. Soc.*, **128**, 15756 (2006); https://doi.org/10.1021/ja064884j
22. D.D. Evanoff Jr. and G. Chumanov, *ChemPhysChem*, **6**, 1221 (2005); https://doi.org/10.1002/cphc.200500113
23. A.H. Alshehri, M. Jakubowska, A. Mlozniak, M. Horaczek, D. Rudka, C. Free and J.D. Carey, *ACS Appl. Mater. Interfaces*, **4**, 7007 (2012); https://doi.org/10.1021/am3022569
24. M.R. Bindhu and M. Umadevi, *Spectrochim. Acta A Mol. Biomol. Spectrosc.*, **135**, 373 (2015); https://doi.org/10.1016/j.saa.2014.07.045
25. W.A. Shaikh, S. Chakraborty, G. Owens and R.U. Islam, *Appl. Nanosci.*, **11**, 2625 (2021); https://doi.org/10.1007/s13204-021-02135-5
26. K.M. Abou El-Nour, A.A. Eftaiha, A. Al-Warthan and R.A. Ammar, *Arab. J. Chem.*, **3**, 135 (2010); https://doi.org/10.1016/j.arabjc.2010.04.008
27. J. Singh, A. Mehta, M. Rawat and S. Basu, *J. Environ. Chem. Eng.*, **6**, 1468 (2018); https://doi.org/10.1016/j.jece.2018.01.054
28. G. Bhumi, M.L. Rao and N. Savithramma, *Asian J. Pharm. Clin. Res.*, **8**, 62 (2015).
29. K. Jyoti and A. Singh, *J. Genet. Eng. Biotechnol.*, **14**, 311 (2016); https://doi.org/10.1016/j.jgeb.2016.09.005
30. L. Wang, F. Lu, Y. Liu, Y. Wu and Z. Wu, *J. Mol. Liq.*, **263**, 187 (2018); https://doi.org/10.1016/j.molliq.2018.04.151
31. S.S. Royji Albeladi, M.A. Malik and S.A. Al-thabaiti, *J. Mater. Res. Technol.*, **9**, 10031 (2020); https://doi.org/10.1016/j.jmrt.2020.06.074
32. S.P. Kumar, P. Darshit, P. Ankita, D. Palak, P. Ram, P. Pradip and S. Kaliaperumal, *Afr. J. Biotechnol.*, **10**, 8122 (2011); https://doi.org/10.5897/AJB11.394
33. V.P. Veeraraghavan, N.D. Periadurai, T. Karunakaran, S. Hussain, K.M. Surapaneni and X. Jiao, *Saudi J. Biol. Sci.*, **28**, 3633 (2021); https://doi.org/10.1016/j.sjbs.2021.05.007
34. M. Oves, M. Ahmar Rauf, M. Aslam, H.A. Qari, H. Sonbol, I. Ahmad, G. Sarwar Zaman and M. Saeed, *Saudi J. Biol. Sci.*, **29**, 460 (2022); https://doi.org/10.1016/j.sjbs.2021.09.007
35. D. Surendhiran, A. Sirajunnisa and K. Tamilselvam, *Environ. Chem. Lett.*, **15**, 367 (2017); https://doi.org/10.1007/s10311-017-0635-1
36. J.L. Smith and P.M. Fratamico, Foodborne Diseases, Academic Press, Elsevier, Amsterdam, p. 189 (2017).
37. M. Prabakaran, V. Hemapriya, S.H. Kim and I.M. Chung, *Arab. J. Sci. Eng.*, **44**, 169 (2019); https://doi.org/10.1007/s13369-018-3398-5
38. S.K. Das, P. Sengupta, M.S. Mustapha, A. das, M.M. Rahman Sarker and M. Kifayatullah, *J. Appl. Pharm. Sci.*, **5**, 57 (2015); https://doi.org/10.7324/JAPS.2015.58.S9
39. K.P. Singh, A. Shyam Kumar, M. Paniteja and S. Singh, *SN Appl. Sci.*, **1**, 741 (2019); https://doi.org/10.1007/s42452-019-0773-0
40. B. Athanassiadis, P.V. Abbott, N. George and L.J. Walsh, *Aust. Dent. J.*, **54**, 141 (2009); https://doi.org/10.1111/j.1834-7819.2009.01107.x

41. E. Jonasson, E. Matuschek and G. Kahlmeter, *J. Antimicrob. Chemother.*, **75**, 968 (2020); https://doi.org/10.1093/jac/dkz548
42. Aryan, Ruby and M.S. Mehata, *Chem. Phys. Lett.*, **778**, 138760 (2021); https://doi.org/10.1016/j.cplett.2021.138760.
43. S. Jain and M.S. Mehata, *Sci. Rep.*, **7**, 15867 (2017); https://doi.org/10.1038/s41598-017-15724-8
44. H. Munir, A. Mumtaz, R. Rashid, J. Najeeb, M.T. Zubair, S. Munir, M. Bilal and H. Cheng, *J. Mater. Res. Technol.*, **9**, 15513 (2020); https://doi.org/10.1016/j.jmrt.2020.11.026
45. L.R.B. Elton and D.F. Jackson, *Am. J. Phys.*, **34**, 1036 (1966); https://doi.org/10.1119/1.1972439
46. G. Dhanaraj, K. Byrappa, V. Prasad and M. Dudley, Springer Handbook of Crystal Growth, Springer, Berlin Heidelberg, p. 32 (2010).
47. D.M. Mott, N.T. Mai, N.T. Thuy, T. Sakata, K. Higashimine, M. Koyano and S. Maenosono, *J. Phys. Chem. C*, **115**, 17334 (2011); https://doi.org/10.1021/jp205588e
48. A. Arsenlis and D.M. Parks, *J. Mech. Phys. Solids*, **50**, 1979 (2002); https://doi.org/10.1016/S0022-5096(01)00134-X
49. S. Maiti, G. Barman and J. Konar Laha, *Appl. Nanosci.*, **6**, 529 (2016); https://doi.org/10.1007/s13204-015-0452-4